Author/s:
Volino, RJ;Fritsch, D;Devenport, WJ;Eca, L;Garcia-Mayoral, R;Mckeon, B;Piomelli, U;Chung, D;Vishwanathan, V;Kerkvliet, M;Toxopeus, S;Hutchins, N

Title:
Effects of roughness on non-equilibrium turbulent boundary layers

Date:
2024-11-01

Citation:
Volino, R. J., Fritsch, D., Devenport, W. J., Eca, L., Garcia-Mayoral, R., Mckeon, B., Piomelli, U., Chung, D., Vishwanathan, V., Kerkvliet, M., Toxopeus, S. & Hutchins, N. (2024). Effects of roughness on non-equilibrium turbulent boundary layers. Journal of Turbulence, 25 (10-11), pp.369-385. https://doi.org/10.1080/14685248.2024.2360186.

Persistent Link:
https://hdl.handle.net/11343/354828

Effects of roughness on non-equilibrium turbulent boundary layers

Ralph J. Volino[a], Daniel Fritsch[b], William J. Devenport[b], Luís Eça[c], Ricardo García-Mayoral[d], Beverley McKeon[e], Ugo Piomelli[f], Daniel Chung[h], Vidya Vishwanathan[a b], Maarten Kerkvliet[g], Serge Toxopeus[g] and Nicholas Hutchins[h]

[a]United States Naval Academy, Annapolis, MD, USA; [b]Virginia Tech, Blacksburg, VA, USA; [c]Universidad Lisboa, Lisbon, Portugal; [d]University of Cambridge, Cambridge, UK; [e]Stanford University, Stanford, CA, USA; [f]Queen's University, Kingston, ON, Canada; [h]University of Melbourne, Parkville, VIC, Australia; [g]Maritime Research Institute Netherlands (MARIN), Wageningen, The Netherlands

ARTICLE HISTORY
Compiled May 23, 2024

ABSTRACT
The effects of roughness were considered as part of a NATO Advanced Vehicle Technology effort titled "Non-Equilibrium Turbulent Boundary Layers at High Reynolds Numbers" (NATO AVT-349). This paper comments on the current state of understanding of the flow physics and modeling efforts to predict rough-wall boundary layer behavior. Outer layer similarity to smooth wall flows and Reynolds number effects are discussed for zero, favourable, and adverse pressure gradients based on the results of experiments and numerical simulations. Various types of modeling are considered including Reynolds averaged Navier-Stokes (RANS) models with different roughness and turbulence models, wall-modeled large eddy simulations (WMLES), and resolvent models. Current needs and gaps in present understanding are discussed along with recommendations for future experiments and computations.

1. Introduction

Roughness can have a strong effect in increasing drag. Applications of interest include naturally occurring flows such as the atmospheric boundary layer and engineering applications such as the flows over aircraft and naval vessels, and the flows over airfoils and other lifting surfaces, including those in turbomachinery and the appendages on ships and submarines. Predicting the effect of roughness on boundary layers is, therefore, of great interest and importance. Predictive capabilities are generally good for canonical, zero pressure gradient (ZPG) boundary layers with homogeneous roughness, which have been well studied, but less is known about non-ZPG flows and non-equilibrium cases with changing roughness or pressure gradients. Such flows are important since canonical conditions occur in only a subset of the flows of interest.

The existing state of knowledge was discussed in the position paper of Volino et al. [1]. They noted that the relationship between the roughness function ΔU^+ (the downward displacement of the mean velocity profile in inner coordinates, which is a measure of the increase in drag compared to a smooth wall case), the equivalent

CONTACT R. J. Volino. Email: volino@usna.edu

sandgrain roughness, k_s, and the physical geometry of a rough surface, plays a critical role in any predictive method.[1] Modelers tend to assume that relationships between ΔU^+ and k_s found under equilibrium conditions will apply in non-equilibrium flows, but the accuracy of this assumption has yet to be fully tested or confirmed. They noted the need for new experiments and simulations under realistic roughness conditions to advance the physical understanding of rough-wall flows, and noted the challenges of such work. They also noted the challenges of incorporating improved understanding into predictive models, and observed that the use of the single parameter k_s, which is current practice, may not be sufficient for strong non-equilibrium conditions and that other methods may need to be developed.

The present paper presents new developments, questions, and recommendations that go beyond those of Volino et al. [1]. The work of AVT-349 included physical experiments in multiple facilities, large eddy (LES) and direct numerical (DNS) simulations of smooth- and rough-wall boundary layer flows, Reynolds averaged Navier Stokes (RANS) computations, and lower order modeling (resolvent analysis). The objectives were to build physical understanding of rough-wall boundary layers through the experiments and numerical simulations, and then to use the resulting knowledge and data sets to test and assess existing models and computational methods. The present paper presents some of the results of this work, focusing on new findings, shortcomings discovered in existing methods and knowledge, and recommendations for future work to address the remaining challenges. We restrict our discussion to two-dimensional flows, which have been the focus of the great majority of the investigations so far. The discussion below begins with brief comments on present methods for drag prediction, followed by the findings from experiments and numerical simulations. Roughness modeling and prediction are then considered, followed by a summary of important questions and recommendations.

2. Drag prediction using k_s

The primary need when considering roughness is to predict the drag penalty. To do this it is useful to consider what changes and what stays the same relative to smooth wall boundary layers. For equilibrium ZPG conditions, Townsend [2] indicated that flow quantities in the outer part of the boundary layer, when normalized using the wall friction velocity, u_τ, and the boundary layer thickness, δ, are similar in smooth- and rough-wall cases. Differences are observed in the so-called roughness sublayer, which extends a few roughness heights from the wall. Similarity has been found to be robust for a wide range of flows and roughness types, as noted in reviews such as Jiménez [3] and Chung et al. [4]. When similarity holds, well established smooth wall models for boundary layers can be used for predictive purposes with the roughness effect entering only through the boundary condition at the wall. For equilibrium ZPG cases, the roughness effect is typically expressed in terms of k_s, which is a hydrodynamic quantity equal to the height of monodisperse sandgrain that would produce the same drag penalty as a given rough surface. Given k_s one can predict the drag for fully rough conditions (when the wall friction is due primarily to form drag on the roughness elements as opposed to viscous shear). Determining k_s for an arbitrary rough surface with geometric roughness height k_g, however, is not trivial. Correlations as reviewed in Flack and Chung [5] and more recently data driven methods such as Jouybari et

[1]Here we use k_g to indicate the geometric roughness height (k_g^+ in wall units) and k_s (and k_s^+) to denote the equivalent sandgrain roughness.

al. [6] are typically used to estimate k_s, but these are all *a posteriori* methods in the sense that they rely on existing drag measurements for specific surfaces, and it is sometimes necessary to have estimates for roughness geometries that are outside of the region of parameter space where these methods can be applied with confidence. This is illustrated in Figure 1. Different correlations, as portrayed in panels (b)-(d), provide similar estimates in the parameter-space regions where there is an abundance of data. (Even so, discrepancies in form among the correlations remain noticeable in these data-abundant regions, presumably due to the distribution of fitting data.) However, some biofouling roughness, including barnacles and tubeworms, lie in a region of parameter space -in this case effective slope ES and skewness Sk (circled in Figure 1) - which is relatively unexplored. As a result, the existing methods can provide significantly different predictions in these regions.

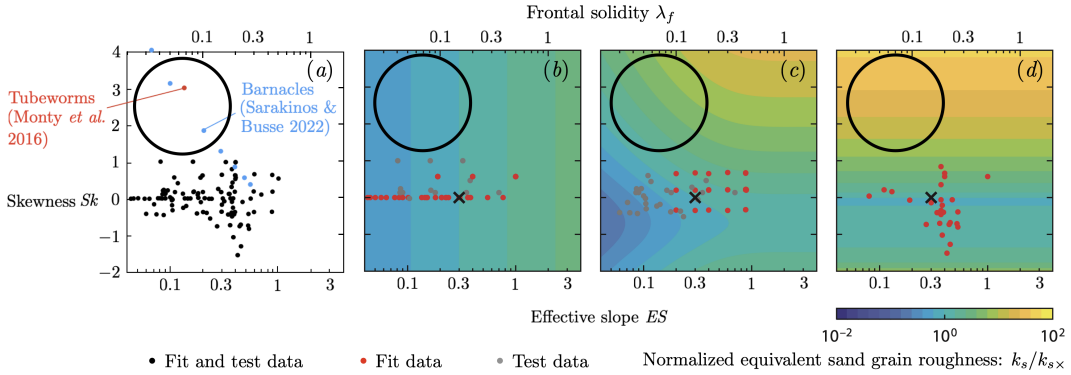

Figure 1. (a) Roughness geometries in the database collected in [4] (combination of all the fit and test data in b-d) as a function of their effective slope/frontal solidity and skewness. A posteriori predictions for the equivalent sand-grain roughness using different data and methods from (b) Chan et al. [7], (c) Forooghi et al. [8] and (d) Flack et al. [9]. The normalizing quantity $k_{s\times}$ is the value for each correlation when ES=0.3 and Sk=0. Figure adapted from [4]

An expansion of the existing database and the inclusion of additional parameters beyond ES and Sk could be helpful, but the lack of confidence in *a posteriori* predictions for undocumented roughness topologies calls for *a priori* methods that can apply even when relevant drag data are missing. In order to develop these, we argue that it is necessary to gain a good understanding of the physical mechanisms that result in the increase in drag. Such methods may be even more important when considering transitionally rough and non-equilibrium cases, as will be discussed further below.

3. Experimental studies and numerical simulations

3.1. Non-zero pressure gradients

Experiments were conducted with changing pressure gradients at Virginia Tech (VT) and the U. S. Naval Academy (USNA) under a range of conditions that included favourable (FPG), adverse (APG) and zero (ZPG) pressure gradient regions.

Experiments at VT studied a high $k_g^+ = k_g u_\tau/\nu$ (>300) regularly-patterned surface of staggered roughness elements under the influence of a family of bidirectional, continually varying pressure gradients. The study was performed in the hard-wall configuration of the hybrid-anechoic test section of the Virginia Tech Stability Wind Tunnel, a low Mach number, high Reynolds number, low turbulence intensity facil-

ity. The pressure gradient family was produced by a 0.914 m chord NACA0012 airfoil mounted across the full 1.85 m span of the tunnel, displacing repeatable pressure gradient distributions onto the wall-mounted rough surface consisting of 2 mm high circular cylinders. Static pressure/pressure gradient distributions, mean velocity profiles, 2D 3-component time-resolved particle image velocimetry (PIV), and fluctuating surface pressure were measured, in addition to various reference tunnel conditions. Skin friction over the rough wall was estimated using the modified Clauser method, as described in Perry & Joubert [10]. This method also provided an estimate of the Hama roughness function, ΔU^+, from which the effective roughness parameter was determined using Nikuradse's model, $\Delta U^+ = \frac{1}{\kappa} ln(k_s^+) + 3.5$, where κ is the von Kármán constant taken to be 0.41. Uncertainty of the k_s/k_g ratio was determined by iterating the method through multiple permutations of plausible logarithmic extents which were selected via a logarithmic-law diagnostic function (see Osterlund et al. [11]). Within the 95 % confidence interval, the k_s/k_g was approximately 1.60, constant and independent of pressure gradient variation. Further discussions of this process and the effectiveness and sensitivity of this method are discussed in Vishwanathan et al [12]. More details on the VT experiments can be found in Fritsch et al. [13] as well as Fritsch [14] and Vishwanathan [15].

Experiments at USNA documented the boundary layer on a wall with mathematically generated random roughness which was fabricated using additive manufacturing. The rough surface formed the flat floor of a water tunnel. The ceiling was adjustable to set the desired pressure gradient in the test section. Baseline cases were measured with a ZPG along the length of the test section using three different inlet velocities. Cases were then documented for three different positions of the ceiling and the same three inlet velocities. In all of the non-ZPG cases, an initial ZPG region was followed by an FPG, a second ZPG region where the flow recovered to canonical conditions, and an APG region. In the various cases, the acceleration parameter, $K = (\nu/(U_\infty^2))((\mathrm{d}U_\infty)/\mathrm{d}x)$ where U_∞ is the local freestream velocity, varied from -1×10^{-6} to 2×10^{-6}. The Clauser pressure gradient parameter, $\beta = -(U_\infty \delta^*/u_\tau^2)(\mathrm{d}U_\infty/\mathrm{d}x)$ where δ^* is the displacement thickness, varied from -1 to 65. The friction Reynolds number, $Re_\tau = u_\tau \delta/\nu$, was as high as 4400 in some cases. Fully rough conditions $k_s^+ > 80$ were present for most measurement locations of most cases. Measurements included two-component velocity profiles acquired with laser Doppler velocimetry (LDV) at 12 streamwise stations along the centerline of the test section for each case. Mean velocity, Reynolds stresses, and higher order moments were documented. Friction velocities were determined from the LDV data using the method of Volino and Schultz [16], which utilizes the mean streamwise velocity and Reynolds shear stress profiles. Planar PIV was used to document flow fields in the streamwise-wall normal and streamwise-spanwise planes at the same 12 measurement stations for each case. The rough-wall cases are presented in Volino and Schultz [17, 18] and a full set of smooth-wall comparison cases are shown in Volino [19, 20]. The LDV profile data from the smooth- and rough-wall cases as well as the test section geometry and detailed coordinates of the rough surface are available as an entry in the roughnessdatabase.org at the University of Southampton.

Results from both the VT and USNA experiments indicate that there is Reynolds number independence for rough wall flows. An example is shown in Figure 2 from Volino and Schultz [18]. The largest difference between the rough- and smooth-wall cases in the figure (in the near-wall Reynolds shear stress profiles at Station 9) is only slightly outside the experimental uncertainty bands. Reynolds number independence has been shown in many studies for ZPG conditions on rough walls and is expected

under fully-rough conditions since the drag at the wall is due to form drag as opposed to viscous shear. The non-ZPG results, therefore, are not surprising, but are new. They potentially limit the parameter space needed for future work by removing the need to vary the inflow velocity in experiments and computations.

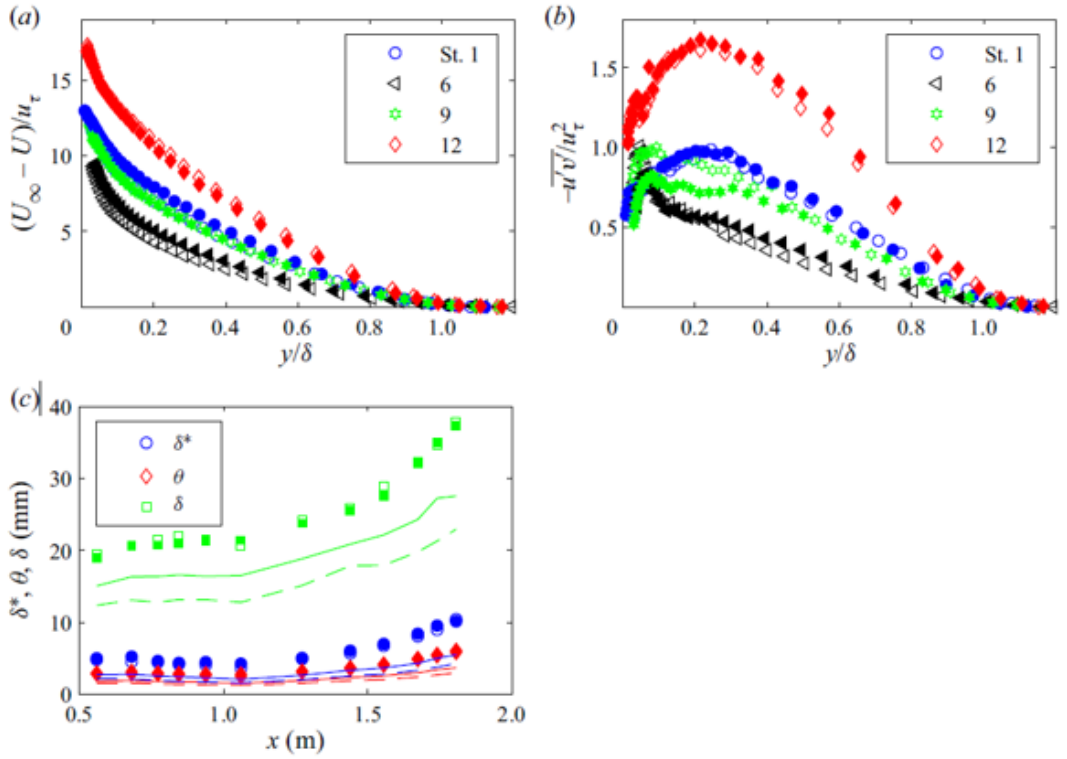

Figure 2. Data from moderate pressure gradient cases of [18] showing Reynolds number independence: (a) mean velocity profiles at stations (St.) 1, 6, 9 and 12 at end of initial ZPG, FPG, ZPG recovery and APG regions; (b) Reynolds shear stress profiles; (c) boundary layer thicknesses. Open symbols from the $U_{\infty,o} = 0.5$ m/s case, solid symbols from the $U_{\infty,o} = 2$ m/s case. Lines show values for corresponding smooth-wall cases with colours corresponding to quantities in the legend, solid lines for the $U_{\infty,o} = 0.5$ m/s case, dashed lines for $U_{\infty,o} = 2$ m/s case. Figure from [18]

The non-ZPG results from both VT and USNA show that when the freestream velocity distribution is matched between smooth- and rough-wall cases, which is equivalent to matching the streamwise variation of K, outer layer similarity largely holds in FPG regions. In an FPG, β values remain small because u_τ tends to be large and boundary layer growth is reduced or reversed so δ^* is typically small. On a smooth wall, a constant K FPG is a sink flow that will approach complete equilibrium in both the inner and outer boundary layer. The rough-wall cases studied also appeared to approach a similar equilibrium in the outer region, but they proceeded through the transition between the ZPG and FPG equilibrium somewhat faster than the comparable smooth-wall cases. This may have been due to higher turbulent mixing with the rough-wall. For the cases considered, the boundary layer thickness remained large compared to the roughness height, but for sink flow conditions with uniform roughness, the ratio of δ/k_s becomes increasingly small, so that a true equilibrium cannot be reached. Cases in which δ/k_s approaches unity may be of interest in future work. Although not a condition that would be expected in practice, a case in which k_g decreased in the

streamwise direction such that δ/k_g remained constant with a constant K FPG could conceivably be constructed (and would be relatively easy to simulate numerically) and might be of interest for showing similarities and differences between equilibrium sink flows on rough and smooth walls.

The APG results show that when the freestream velocity distribution is matched, outer layer similarity does not appear to hold as large differences were observed between rough- and smooth-wall cases. In hindsight, this is not surprising since the boundary layer grows much faster and the skin friction coefficient drops more quickly on rough surfaces, resulting in much higher β for the rough case. It should also be noted that the similarity observed in ZPG and FPG boundary layers noted above was for cases that did not include an upstream APG. When following an APG region, an immediate return to similarity cannot be expected, as shown in Vishwanathan et al. [12]. Rough- and smooth-wall cases from Volino and Schultz [18] with different configurations and K values but β of similar magnitude suggest that outer layer similarity may hold if the β history is matched. This is only a preliminary conjecture, however, since cases with the same history were not measured. More work is needed and recommended to explore this.

There is no evidence from any of the experiments that k_s changes with the pressure gradient. This is an encouraging and useful result, as the assumption of a constant k_s for a given surface is assumed in current modeling methods. It is only a preliminary result, however, based on the limited data available. There is some preliminary evidence that the relationship between ΔU^+ and k_s may change as δ/k_s becomes small. This can be the case in FPG flows, but Volino and Schultz [17] also observed it under ZPG conditions and indicated that it may be a concern when $\delta/k_s < 30$. This is consistent with the observation of Jiménez [3] that as δ/k_s becomes small, the flow becomes more like that over obstacles than roughness. Still, experiments to determine k_s for a given surface are sometimes done when $\delta/k_s < 30$, so further investigation of such cases is recommended.

3.2. Transitionally rough cases

For a given roughness geometry, once the roughness size in viscous units, k_s^+, is large enough that the surface behaves as fully rough, the evolution of ΔU^+ with k_s^+ is generally understood to become universal (e.g. Chung et al. [4]), at least for equilibrium ZPG cases. The problem however is that k_s needs to be known in advance to define this universal regime, and the transitionally rough regime itself can be of interest in some applications. It is, therefore, of interest to understand the non-universal behaviour of ΔU^+ with roughness size k_g^+ up to the point where the fully rough regime sets in, at which point the ratio k_s/k_g can be established. This regime has been investigated at the University of Cambridge (Abderrahanam-Elena et al. [21], Mulchadani and García-Mayoral [22]), through a set of direct simulations for the VT roughness geometry [13] as portrayed in Figure 3, in the range $k_g^+ \approx 5$–60, which for this geometry results in $\Delta U^+ \approx 1$–10, thus ranging all the way from the hydraulically smooth to the fully rough regime.

In the immediate vicinity of the wall, the flow must follow the surface topology, leading to a component of the flow that is coherent with the roughness geometry, exhibiting a signature of the texture clearly and sharing its length scales. Its intensity can be characterized well by the dispersive flow, the temporal average of the flow that exhibits the spatial signature of the texture. The remaining component of the flow,

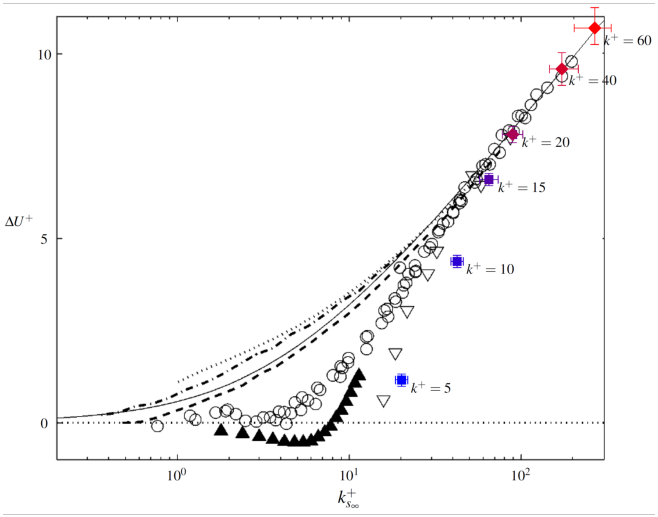

Figure 3. Roughness function ΔU^+ as a function of the roughness size in viscous units, expressed in terms of equivalent sand-grain roughness k_s^+. Coloured symbols are for the DNSs from [22]. Black symbols and lines are from Jiménez [3]

which would exhibit no texture signature, is the background, texture-incoherent turbulence. The analysis of the above simulations highlights the importance of the interplay between the texture-coherent flow and the background, texture-incoherent turbulence, as previously suggested for superhydrophobic textures in Fairhall et al. [23] and recently corroborated in Xie et al. [24]. Figure 4 portrays spectral density maps for the three velocity components and shear Reynolds stress for the DNS cases displayed in Figure 3, showing how the texture harmonics, representative of the texture-coherent component of the flow interact with the background-turbulence component and modify it, particularly for intermediate roughness sizes. Due to the non-linearity of the advective terms, this interaction is broadband in lengthscales, and in the cases portrayed results in energetic regions arising in the spectral maps at shorter and somewhat wider streamwise and spanwise lengthscales, compared to smooth-wall turbulence. Work is currently underway to investigate if the effect of the surface texture can be reduced to the non-linear interaction between these two flow components, and how this interaction affects the background-turbulence component, not only for the simple case of slip/no-slip textures of [23] and [24] but also for the more general case of rough textures. To capture the interaction accurately, it is particularly important to retain the modulation in amplitude caused by the overlying, texture-incoherent turbulence on the near-wall, texture-coherent flow, as proposed in [21]. This requires an extension of conventional triple decomposition [25] to account for the modulation effect.

3.3. Additional cases

Experiments were conducted at the University of Melbourne for ZPG boundary layers with streamwise strips of roughness with smooth regions between the roughness strips, as presented in Wangsawijaya et al. [26]. The width of the roughness strips was varied, and the effect of the spacing on the secondary flows at the interfaces between the smooth and rough regions was documented. The effects of roughness on scalar transport was investigated using direct numerical simulations of flow over homogeneous random roughness in a ZPG boundary layer as reported by Hantsis and Piomelli [27].

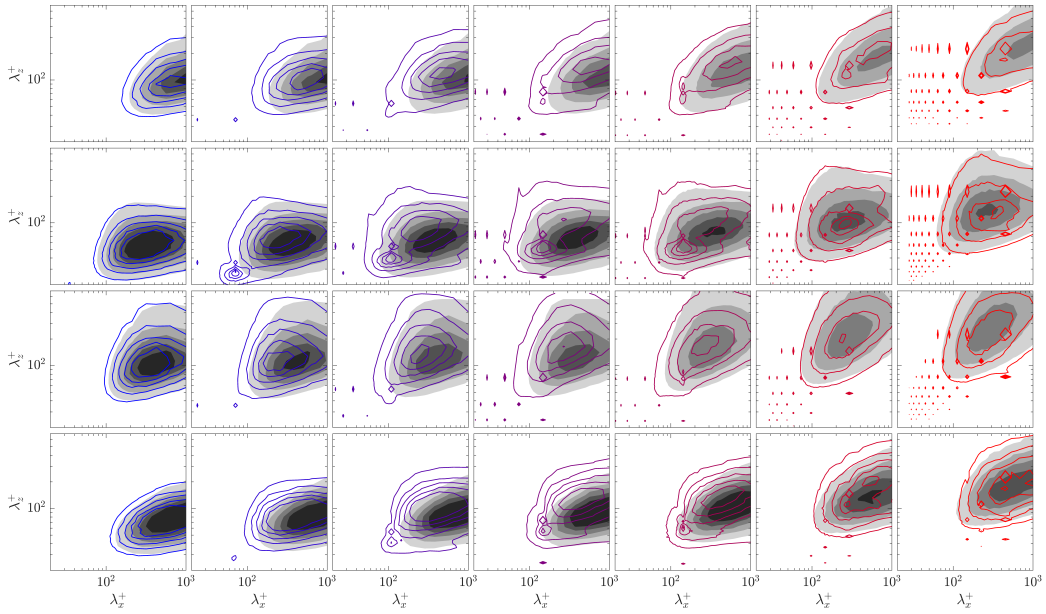

Figure 4. Spectral energy densities over the regular roughness of [10] at a plane roughly 4 viscous units above the roughness tips, from left to right and blue to red for roughness sizes from $k_g^+ \approx 5$, 10, 16, 21, 21, 43 and 65. The first four cases were run at $Re_\tau \approx 190$, and the last three at $Re_\tau \approx 380$. Note that simulations for $k_g^+ \approx 21$ were run at both Reynolds numbers. The first row portrays the premultiplied energy spectrum of the streamwise velocity, the second row that of the wall-normal velocity, the third row that of the spanwise velocity, and the fourth row the cospectrum of the uv shear Reynolds stress. The shaded contours are for a reference smooth-wall flow.

An immersed boundary condition was used to model the roughness. These studies are described in their respective references and are mentioned here because the data generated were used in the modeling efforts described below.

4. Modeling

4.1. Reynolds averaged Navier Stokes (RANS) computations

4.1.1. Overview of roughness models for RANS

The original proposal to take into account roughness effects was presented by Wilcox [28] and it corresponds to a change of the ω wall boundary condition ω_w that depends on k_s. This simple model can be applied to the several versions of the $k-\omega$ model proposed by Wilcox [29] and to the Turbulent-non-Turbulent (TNT) version proposed in [30]. However, when applied to the Shear-Stress Transport (SST) versions of the $k-\omega$ model [31, 32] its effect is cancelled by the limiter included in the definition of the eddy-viscosity [33]. An extra damping function is required in the definition of the limiter of the eddy-viscosity to apply roughness effects in the SST $k-\omega$ model with the Wilcox approach [33].

Alternatives to the Wilcox approach that rely on the k and ω wall boundary conditions (k_w and ω_w) are presented in [34] and [35]. The alternatives presented in [35] are based on roughness functions with (Nikuradse) or without (Colebrook) an inflexion point in the roughness function for the transitional roughness regime. These three roughness models can be applied to the SST $k-\omega$ models without any modification

of the limiter of the eddy-viscosity definition. Figure 5 illustrates the wall boundary conditions of k and ω of these roughness models as a function of k_s in wall coordinates.

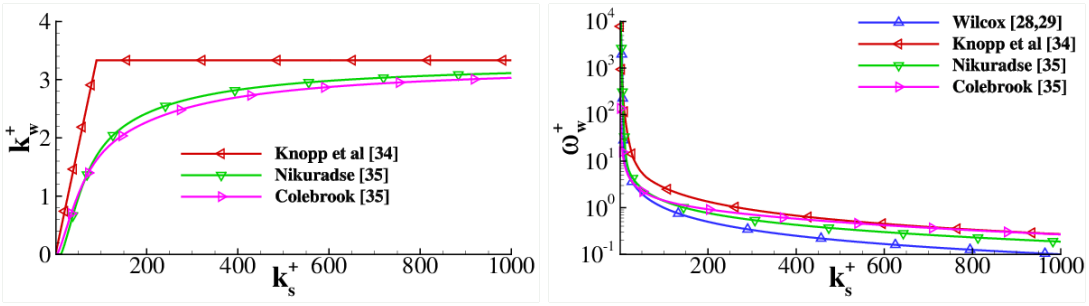

Figure 5. k and ω wall boundary conditions for the roughness models proposed in [28, 29, 34, 35]

A general technique to include roughness effects in eddy-viscosity models is proposed in [36]. The technique is illustrated for the $k - L$ model [37]. Its adaptation to the $k-\sqrt{k}L$ model [38] is presented in [39]. When compared to the $k-\omega$ roughness models mentioned above, the main difference is the change of the calculation of the distance to the wall that requires a non-zero wall value d_w that depends on k_s. The roughness models based on k_w and ω_w can also be adapted to the $k - \sqrt{k}L$ model [39].

Another alternative to the Wilcox formulation is the hydrodynamic roughness length proposed in [40] for two-layer wall models. An empirical calibration relates k_g to ΔU^+ and a hydrodynamic roughness length. The introduced length scale is then used to modify the turbulence length scale and k boundary condition, thus simulating the effect of the rough wall.

Roughness models can also be incorporated in the Spalart-Allmaras, one-equation, eddy-viscosity model [41]. The two proposals presented in [31, 42] change the wall value of the undamped eddy-viscosity, $\tilde{\nu}$, and shift the distance to the wall by a non-zero value at the wall d_w. The Boeing proposal [43] uses Neumann boundary conditions at the wall and a value of d_w that does not depend on the friction velocity at the wall, but it requires changes in the $\tilde{\nu}$ transport equation. The Aupoix approach imposes $\tilde{\nu}$ and d_w at the wall, with both quantities depending on k_s^+. The d_w^+ function presented in [43] is different from that given in [42]. As illustrated in Figure 6, the equation presented in [43] seems to be incorrect, because it gives negative values of d_w^+ up to $k_s^+ = 3.54$ and it is clearly below the equation presented in [42] that is close to the proposal of [36] in the transitional roughness regime.

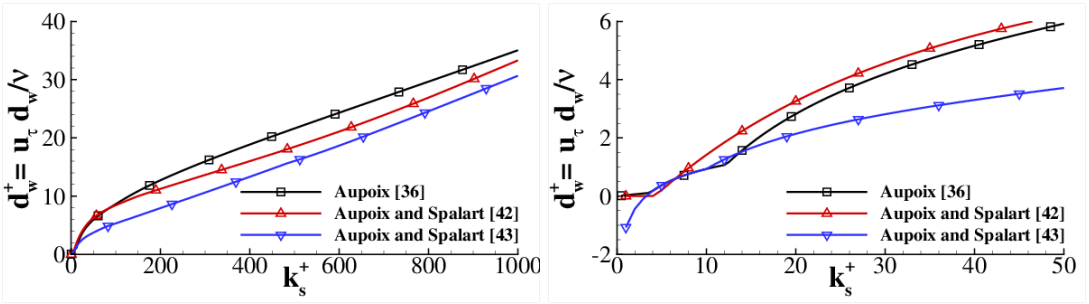

Figure 6. Shift of the distance to the wall d_w as for the roughness models proposed in [36, 31, 42]

There are no roughness models proposed in the open literature for Reynolds-stress

models. Nonetheless, the Wilcox approach [28] can be easily tested in the SSG-LRR$-\omega$ Reynolds stress model [44] that uses an ω transport equation to determine the dissipation rate. However, it is not clear if extra damping functions, as for the $k-\omega$ SST model, and/or the shift of the distance to the wall is required. It seems logical that a non-linear model, particularly one which could incorporate non-locality, would produce more accurate and consistent simulation results with better k_s matching, but such hypotheses require further investigation.

4.1.2. MARIN/IST RANS computations

Computations were done at Virginia Tech and in a collaboration between the Maritime Research Institute Netherlands and the Instituto Superior Tecnico of Lisbon (MARIN/IST). Both groups used two-dimensional steady RANS to simulate the VT experimental flow cases. Both used the k_s value obtained from the experiments for the rough surface to impose the wall boundary condition. Neither used wall models or resolved the roughness elements.

The MARIN/IST work is based on previous studies [45, 46, 47, 39] and new simulations of the VT experiments. Several problems were encountered for the comparison between experiments and simulations: the computational domain suggested for the smooth wall simulations [48] was used, but there was a clear mismatch between measurements and simulations at the first measured station; the rough wind-tunnel wall starts at the same location as the simulations, but it extends all the way to the outlet station, which is not identical to the experiments. Therefore, it is difficult to make a meaningful comparison between experiments and simulations. Nonetheless, it is possible to assess the effect of non-equilibrium pressure gradients and scale effects.

The results obtained for flat plate ZPG boundary layers with the several combinations of turbulence and roughness models mentioned above show different trends in the solutions. In the $k-\omega$ models, the Wilcox (with the additional blending function for the SST versions) [29], Knopp et al. [34] and Colebrook approaches lead to similar results for the fully-rough regime [47], which are in good agreement with the Mills and Hang correlation [49]. On the other hand, the Nikuradse roughness model is more appropriate for the transitional roughness regime [35, 49], where the poorest results are obtained with the Knopp et al. approach [35, 49]. As expected [35], the Colebrook approach does not exhibit any inflexion point in the roughness function for the transitional regime.

Preliminary results obtained for the $k-\sqrt{k}L$ model [39] show similar trends to those discussed above for the $k-\omega$ models. However, the specification of the shift of the distance to the wall d_w has a significant influence on the results. On the other hand, up to values of k_s^+ close to 80, the SSG-LRR$-\omega$ Reynolds-stress model (RSM) [44] combined with the Wilcox roughness model [29] leads to very similar results to those obtained with the same roughness model combined with the SST $k-\omega$ model. For larger values of k_s^+ the solution of the RSM model deteriorates, which can be a consequence of the behaviour of the blending function of the model that depends on the distance to the wall.

The results obtained in [46] and [47] also show that the increase of k_s makes the slope of the log-law region obtained with the $k-\omega$ models closer to the expected value of $\kappa = 0.41$, when compared to the smooth wall solution. However, as discussed below, this effect tends to diminish with the increase of the Reynolds number.

Calculations of the VT rough wall experiments were performed with several combinations of the turbulence and roughness models mentioned above. The simulations

made at the experimental Reynolds number of Re $= 2 \times 10^6$ showed significant effects of the pressure gradient on the mean velocity profiles of the wind-tunnel wall boundary-layer. As for the smooth wall simulations [50], the slope of the log-law region is strongly dependent on the pressure gradient. Furthermore, in the regions of largest variation of the pressure gradient parameter, it is hard to define the limits of the log-law region because, it is troublesome to detect a region with a constant mean-velocity slope diagnostic function.

As for the smooth wall case [50], the simulations of the Virginia Tech rough-wall experiments were also performed for a Reynolds number of $Re = 10^9$. The differences between the solutions obtained with different turbulence and roughness models are much smaller than those observed at Re $= 2 \times 10^6$. Furthermore, the effect of the pressure gradient on the mean velocity profiles is much weaker than that observed for Re $= 2 \times 10^6$.

4.1.3. VT RANS computations

For the Virginia Tech computations, results were obtained using the CREATE-AV Kestrel KCFD finite volume solver. Verification and validation efforts of the involved grids and baseline computational methods are described in Fritsch et al. [48]. A roughness boundary condition was applied to the grids along the same extent as in the experiment using a variety of roughness modeling methodologies. A modified Wilcox-style condition produced a non-physical asymptote in the roughness function - roughness Reynolds number relationship, as described in Fritsch et al. [13]. Modifications to the wall condition inspired by the work of Aupoix [35] (among others, see, e.g., Knopp et al. [34]) produced better matching and more robust results at high k_s^+ values, as described in Fritsch et al. [51].

Replicating established rough wall physics, e.g. the $\log(k_s^+) \propto \Delta U^+$ relationship or Townsend's outer layer similarity, in a RANS environment proves challenging and it is still open for debate how best to model rough wall physics within the confines of the RANS equations. The Wilcox-style model of reducing the wall boundary condition dissipation rate of a two-equation turbulence model as a function of k_s^+ can produce reasonable results for small values of k_s^+ but these models produce a horizontal asymptote in the $\log(k_s^+) \propto \Delta U^+$ relation that is not observed experimentally (Figure 7 from Fritsch et al. [51]). Fritsch et al. [13, 51] hypothesized that this is due primarily to the conceptual non-physicality of the boundary condition: a reduction in dissipation is not the physics at play near a rough wall. More success was found by adapting the model of Aupoix [35] to the Menter SST model [31], which effectively shifts the wall by some wall distance proportional to k_s. A similar modification to the Boeing-Aupoix-Spalart [43] Spalart-Allmaras (SA) roughness model yielded excellent agreement with experiment. The SA and SST models were implemented primarily due to the wide availability and relative computational simplicity of their roughness extensions and for direct practical application; as these models are the most widely utilized in industry, they are the most likely roughness extensions to be employed in a production setting.

It is worth nothing that Knopp et al. [34] observed that the Wilcox model's performance with the Menter SST model for high k_s^+ flows improved with mesh refinement below a first-cell-from-the-wall value of $y^+ = 0.001$. This was due to over-activity of the SST limiter for coarser near wall spacings. The finest mesh in the present study had a near wall spacing of $y^+ \approx 0.08$. While this is a very fine spacing for a typical RANS solution, it is nearly two orders of magnitude higher than the 0.001 suggested

by Knopp et al.

The wall-shifted-smooth-wall-boundary-layer concept of the rough wall boundary layer has received support in the literature (e.g. Kays and Crawford [53], and Durbin and Petterson Reif [54]), but the exact nature is still in question. Fritsch et al. [51] observed that producing experiment-matching results in a RANS environment required a different k_s value than what was measured for the same case experimentally, and that this k_s value was different for the SST and SA models, as shown in Figure 8 from Fritsch et al. [51]. The relationships between geometric k_g, true k_s, turbulence model k_s, and flow physics remains unclear and worthy of future exploration.

One of the most studied aspects of rough wall flows is Townsend's [2] outer layer Reynolds number similarity hypothesis. Under this assumption, it can be observed that a given rough wall boundary layer above the sublayer will collapse on an outer scaling independent of free-stream Reynolds number. The one-equation SA based roughness model captures this behaviour well, as depicted in Figure 9 from Fritsch et al. [51], but the two-equation SST version does not. This does not imply that the SA model is more physically meaningful or accurate than the SST, but it does produce results that are consistently more in line with experimental observations of rough wall behaviour.

These observations raise several questions about the nature of rough wall flows and their modeling. Within the limitation of the RANS equations, what precisely is a rough wall? Results indicate that assuming it is a smooth wall with some finite, non-infinite specific dissipation as in the Wilcox-style scheme is fundamentally incorrect. A smooth wall that has been shifted some distance proportional to k_s appears to be more valid, or at least produces more consistent results. Another possibility yet to be explored is that, under the conditions of wall similarity, the rough wall is essentially equivalent to a smooth wall with a negative slip velocity of magnitude ΔU^+. This thought is intriguing as it functions with existing turbulence models without modification to the modeling parameters, only to the enforced velocity condition at the wall. This would produce meaningless results in the very-near-wall region, but we already currently assume this region is meaningless in a rough wall simulation as there are no roughness geometry or associated local flow effects modeled.

What is the relationship between k_s, the associated roughness effect, and the RANS equations? Current models can qualitatively capture these effects, but require *a priori* knowledge of the true ΔU^+ to ensure accurate matching, which in many ways defeats the purpose of a simulated environment. This is partially due to the complexity and lack of understanding of the geometry-physics relationships at play and partially to a lack of understanding of the physics-RANS equations relationship. There is a great need for modeling strategies that do not require any *a priori* knowledge of the roughness function to be sufficiently useful. This could entail more robust strategies for determining k_s from a given roughness distribution, or it could require a roughness modification for a given distribution that goes beyond the equivalent sandgrain approach.

4.1.4. Further remarks

There are several sand-grain roughness models available in the open literature that can be combined with eddy-viscosity models and even with Reynolds-stress models. Although these models have a common background, the vertical shift of the log-law region ΔU^+, the results depend on the combination of roughness and turbulence model. The quantitative assessment of the modeling accuracy of the several alternatives available requires experimental data obtained in conditions that can be replicated in the

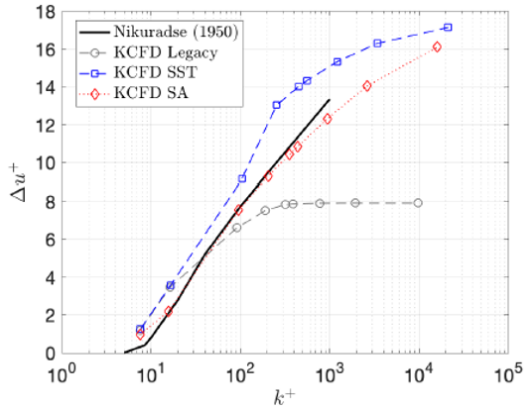

Figure 7. Roughness function as a function of roughness Reynolds number for legacy two-equation and modern Spalart-Allmaras and Menter SST boundary conditions compared with data of Nikuradse [52]. Figure from [51]

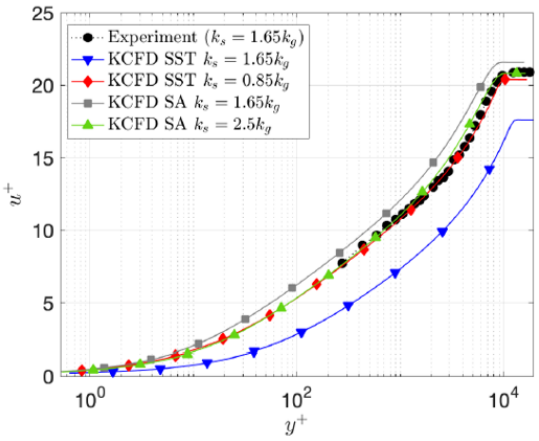

Figure 8. Viscous normalized velocity profiles as measured experimentally and as simulated with SA and SST models using experimental k_s and k_s tuned to match ΔU^+ for the ZPG case. Figure from [51]

simulations, which is not an easy task, especially using two-dimensional simulations. Nonetheless, as for the smooth wall conditions, RANS solutions using the turbulence and roughness models mentioned above are strongly dependent on the Reynolds number, which makes error assessment a challenging task.

All of the above suggests quite strongly that producing an accurate RANS-based prediction of drag on a rough surface within an acceptable confidence level is likely out of reach with the current state-of-the-art and that much further research is required. For high k_s^+ flows, c_f scales directly with k_s, implying that some uncertainty in k_s results in a comparable uncertainty in drag, and the *a priori* uncertainty in an estimated k_s will be high, both due to the lack of accurate roughness correlation models and the observed mismatch in experimental and numerical k_s values.

4.2. Roughness models for LES

Wall-Resolved Large-Eddy Simulations (WRLES) do not require roughness models, as the roughness elements are resolved by the grid. The limitations for DNS/WRLES

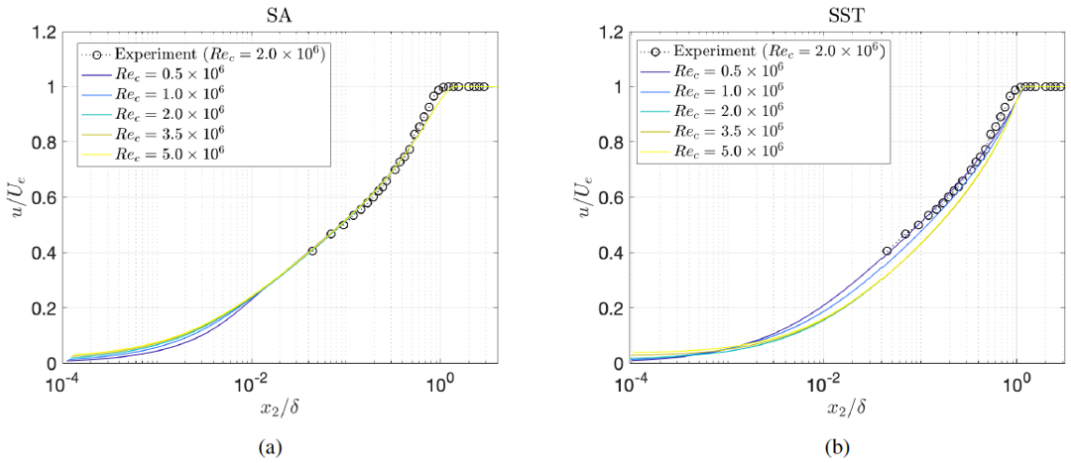

Figure 9. Outer normalized velocity profiles as measured experimentally and as simulated with (a) SA and (b) SST models with constant k_s and increasing free-stream Reynolds number for ZPG case. Figure from [51]

are (1) The Reynolds number, (2) the sample size (i.e. how many roughness elements are there in the computational domain) and (3) the geometry. Every approach has shortcomings: body-fitted grids work for very regular roughness (e.g. egg carton, ribs or cubes). Complicated roughness shapes require suboptimal grids (unstructured, triangular prisms or tetrahedra) that reduce accuracy. Immersed Boundary methods can be used on regular grids. First-order methods (volume of fluid-based) are acceptable if there is uncertainty in the geometry definition (sand grain for instance) but if the geometry is defined more precisely the order of accuracy decreases. The advantages of WRLES are the access to the flow in the sublayer, and the fact that the drag is known and can be separated into form and friction components.

In Wall-Modeled LES (WMLES), in which the near-wall is bypassed, on the other hand, roughness must be included through changes in the relationship used to relate the wall stress to the outer-layer velocity. The most common approach, in WMLES, is to assume that the near-wall layer is in equilibrium, and that the velocity satisfies a logarithmic law, which can be used to obtain the friction velocity given the outer-layer velocity predicted by the LES. This approach can easily be applied to rough-wall cases through appropriate modifications of the log law. A generalized form of this method has recently been proposed by Meneveau [55]. This technique, however, has difficulties dealing with heterogeneous roughness, in which the equilibrium assumption does not hold. The response to sudden changes in roughness height is difficult to predict because local phenomena (sheltering, separation, stagnation, changes in the turbulent dissipation, etc.) may drive the flow behavior. These phenomena are difficult (or impossible) to include when the near-wall layer is completely bypassed. Research in this area is ongoing.

4.3. Lower order (resolvent) models

Resolvent analysis for turbulent flows (McKeon and Sharma [56]) takes as input the mean state and identifies the amplification properties of the linear Navier-Stokes operator (the resolvent), linearized relative to that mean. The term that is nonlinear in the fluctuations is considered to be the input forcing to the resolvent. Singular value

decomposition of the resolvent yields the most dangerous input forcings and the associated output states (the right and left singular functions, respectively), ranked by the corresponding gains (the singular values). Details of the analysis are given in, e.g. McKeon [57].

The resolvent operator is formed with knowledge of the mean field, determination of which is often the objective of studies of rough walls. In this sense, resolvent analysis is a useful tool to give insight into the origin of changes to the flow, and the stresses in particular, relative to smooth wall behaviour (although note that resolvent models that support the assumed mean field are at least conceptually possible). Considerations under the AVT study included the importance of mean profile fidelity for resolvent model, as well as obtaining insight into secondary flows and dispersive stresses as well as modifications to the background, spatio-temporal fluctuations.

We considered a range of data made available through the AVT; we focus here on the isolated effects of roughness and the datasets provided by the Melbourne and Queen's groups (Wangsawijaya et al. [26] and Hantsis and Piomelli [27], respectively). The influence of pressure gradient and flow history on amplification identified via the resolvent is discussed in the companion manuscript on smooth-wall non-equilibrium turbulent boundary layers.

Self-similarity of the resolvent operator for a self-similar mean field input has been explored in the context of smooth wall turbulence (Moarref et al. [58]), and the same concepts apply for rough wall flows in which the outer profile collapses in outer variables. Resolvent modes and gains are identical to their smooth wall counterparts in regimes where the mode support is not contaminated by modifications to the mean profile associated with the roughness sublayer. This has important implications for Townsend similarity of the turbulent fluctuations and, beyond the linear analysis discussed here, for the nonlinear sustaining mechanisms of turbulence.

Aspects of the roughness sublayer itself may be represented in a low-order way. Using resolvent basis functions and a linearized boundary condition, the dispersive stresses are amenable to low order models of a range of fidelities, for example by a least squares fit for resolvent mode weights. Figure 10 shows a reconstruction of the spanwise-varying, time-averaged flow associated with the Wangsawijaya et al. [26] roughness strips, obtained using resolvent modes obtained from a smooth wall mean profile at the relevant friction Reynolds number, four harmonics of the spanwise roughness wavenumber and two resolvent modes for each harmonic. The secondary flow in the core of the channel is very well captured by the resolvent model with eight degrees of freedom, with an error of generally less than 5%. The largest deviation is in the near-wall region above the roughness strips, as would be expected due to the linearized boundary condition.

Secondary flows and dispersive stresses in flows with more complex roughness may also be represented in a reduced order way, truncating either the wavenumbers associated with the rough wall geometry, similar to the approach of Mejia-Alvarez and Christensen [59], the number of resolvent modes as described above, or both. The wake-field from the rough-wall channel flow DNS of Hantsis and Piomelli is compared with resolvent models obtained using a smooth-wall mean flow and 0.0048% and 0.12% of the total degrees of freedom of the DNS in Figure 11.

The purpose of the previously described examples is to show the potential use of resolvent analysis in understanding the effects of roughness on wall turbulence. An obvious connection is to the modeling of rough walls in LES and RANS approaches, as well as to immersed boundary method approaches for rough walls. Depending on the objective, abstracted representations of the effects of roughness on wall flows and/or

data-driven reconstructions of flow fields may be of utility for understanding or modeling purposes. A range of specific configurations and questions are under current consideration; note also the discussion of resolvent modeling of the effects of flow history in Klewicki et al. [60], which describes the AVT-349 work on smooth wall non-equilibrium boundary layers.

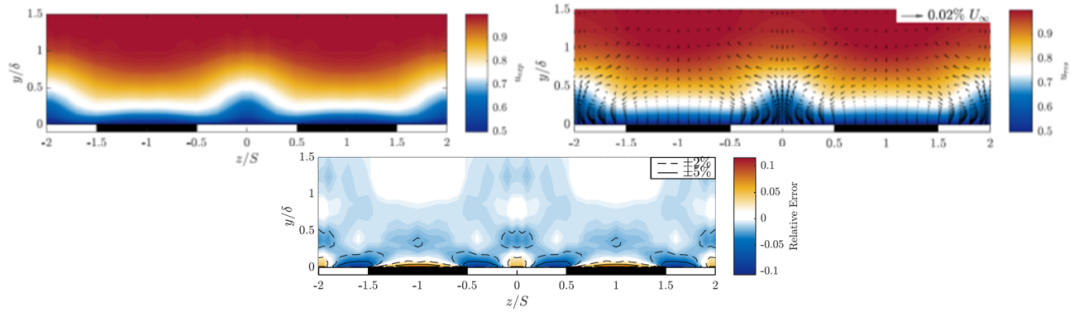

Figure 10. Comparison of the time-averaged streamwise flow in the cross-stream plane from the experiments of Wangsawijaya et al. [26] over spanwise heterogeneous roughness strips (strips of P-36 grit sandpaper and 2 mm thick cardboard of equal width S = 100 mm) with a resolvent model obtained using four harmonics of the spanwise roughness period and two resolvent modes per spanwise harmonic. The black strips represent wall roughness and the white strips show regions of smooth wall. The relative error between the real and modeled flow are shown in the lower panel. Figure courtesy of Yuting Huang, California Institute of Technology

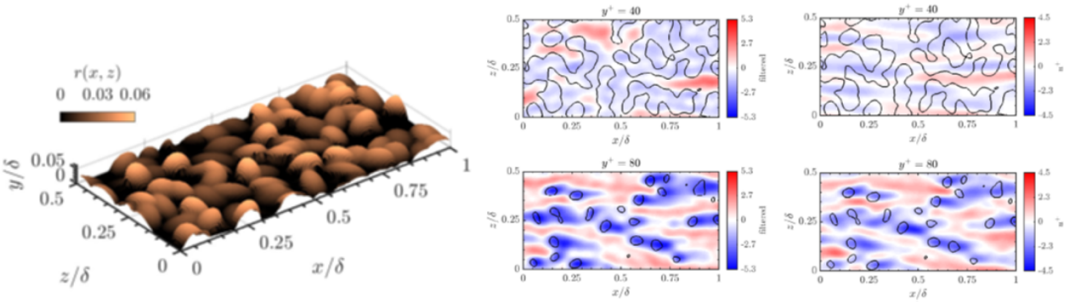

Figure 11. Resolvent representations of the wakefield over the rough wall of Hantsis and Piomelli [27] shown in the left panel. Filtered denotes the streamwise component of the DNS wakefield filtered to remove wavenumbers not included in the resolvent representation, while u' in the righthand column is the resolvent reconstruction obtained using two resolvent modes per spatial wavenumber pair. Figure courtesy of Miles Chan, California Institute of Technology

5. Conclusions, questions and recommendations

A few conclusions can be drawn from the discussion above, but possibly more importantly, the AVT-349 work raises several questions and suggests recommendations for future work to improve our understanding of the flow physics of boundary layers on rough surfaces and the modeling of these flows. Considering the flow physics as investigated through the experiments and numerical simulations:

- Rough surfaces show Reynolds number independence in the outer-normalized velocity profile, turbulence statistics and the outer normalized turbulent pressure

spectrum, at least for fully rough conditions. This appears to be true independent of pressure gradient.

- Townsend's outer layer similarity between rough- and smooth-wall boundary layers appears to largely hold for FPG flows, although the rough-wall cases appear to proceed toward a new equilibrium faster when the pressure gradient is changed. Cases with strong enough FPG to cause relaminarization on smooth walls have not been studied extensively with rough walls. Such cases may be of interest for future work, both with uniform roughness such that δ/k_g decreases in the streamwise direction and with the roughness height, k_g, decreasing such that δ/k_g remains constant.
- The constant δ/k_g case for FPG, ZPG, or APG boundary layers (with k_g increasing or decreasing depending on the pressure gradient) would result in an "equilibrium" roughness. It is recommended that such surfaces be designed and tested with various pressure gradients to separate the effects of variable δ/k_g from other parameters.
- The conditions for testing similarity between rough- and smooth-wall boundary layers has not yet been established. Similarity is not observed for APG flows when the freestream velocity history is matched between smooth- and rough-wall cases. There is preliminary evidence that similarity might be achieved if the β history were the same for rough- and smooth-wall cases. Direct testing of this through experiments or simulations in which different freestream velocity distributions are used to achieve matching β histories for smooth- and rough-wall boundary layers is recommended. Equilibrium cases with constant β and non-equilibrium cases with increasing β are both of interest. Cases approaching boundary layer separation may be of particular practical interest.
- A given rough surface appears to have a singular value of equivalent sandgrain roughness height, k_s, that is not Reynolds number or pressure gradient dependent. This conclusion is based on limited evidence. It should be investigated in future work with different pressure gradients.
- The relationship between k_s and ΔU^+ needs further investigation. Of particular interest are cases that depart from the standard assumptions of fully rough conditions and large δ/k_g.
- We need *a priori* methods to determine k_s for any given rough surface. Existing correlations and data driven methods tend to work adequately for fully rough conditions when confined to the parameter space for which their curve fits or machine learning are based. When extrapolated to other parameter spaces or applied in transitionally rough conditions, existing methods can be insufficient and often disagree with each other. Physics based models, as opposed to curve fits, are needed, which will require a better understanding of how different types of roughness generate drag under different flow conditions. It is recommended that a family (or families) of equal k_s surfaces be designed and tested using different geometries (to determine if/how to separate k_s from geometry and if/how to compute k_s *a priori*).

Considering the modeling efforts:

- The problem of using a 2D simulation to model a physical experiment is essentially the same for rough-wall cases as it is with smooth walls. For a given physical geometry, even if the flow in the center of the test section is free of secondary flows, the presence of side wall boundary layers and corner and junc-

tion flows in an experiment will affect the pressure gradient. Unless somehow adjusted to account for these effects, 2D simulations will miss them.

- RANS models produce the best results when using a k_s dependent wall shift as opposed to a reduction in dissipation at the wall.
- It is recommended that a RANS model using negative wall slip velocities equal to ΔU^+ be built, tested, and validated as an alternative to the wall shift or reduced dissipation methods.
- In the authors' opinion, the available data suggest that RANS models can produce acceptable data, but not at experimental k_s. They require k_s tuning, which requires *a priori* knowledge of the roughness function.
- RANS results depend on the combination of turbulence model and roughness model used. Models vary in their ability to capture outer layer Reynolds number independence, with the Spalart-Allmaras model better than the SST model. This is not necessarily due to how well the models capture the physics. Additional differences are present for flows in the transitionally rough regime.
- We need to develop a better understanding of the relationship between k_s, the roughness effect, and the RANS equations. Current models can work if ΔU^+ is known for a surface, but to be useful, as already stated above, we need physics based models that do not require *a priori* knowledge of the roughness function.
- Resolvent models show considerable promise for building understanding and modeling the effects of roughness on wall turbulence, which aid in the development of the types of *a priori* models needed. Work with resolvent models should continue. They could conceivably be used to model the effect of a given rough surface on the flow in a reduced order way.

Acknowledgements

William Devenport would like to acknowledge the support of ONR, in particular Peter Chang, Ki-Han Kim and Yin Lu Young for their support under grants N00014-18-1-2455, N00014-19-1-2109 and N00014-20-1-2821. Ugo Piomelli acknowledges the support of the Natural Sciences and Engineering Research Council of Canada (NSERC-CRSNG), under the Discovery Grant program. Ralph Volino acknowledges the support of ONR under grant N0001424WX00257 monitored by Peter Chang. Ricardo García-Mayoral acknowledges the support of EPSRC-UK under grant EP/S013083/1 and AFOSR (EOARD) under grant FA8655-22-1-7062. Daniel Chung and Nicholas Hutchins acknowledge support from the ARC and from the AFOSR (AOARD) under grant FA2386-21-1-4018. Beverley McKeon acknowledges support from AFOSR under grant FA9550-21-1-0443 (PM Greg Abate) and ONR grant N00014-17-1-3022.

References

[1] R. J. Volino, W. J. Devenport, and U. Piomelli. Questions on the effects of roughness and its analysis in non-equilibrium flows. Journal of Turbulence, 23(8):454–466, 2022.

[2] A. A. Townsend. The Structure of Turbulent Shear Flow. Cambridge University Press, Cambridge (UK), 1976.

[3] J. Jiménez. Turbulent flows over rough walls. Annual Review of Fluid Mechanics, 36:173–196, 2004.

[4] D. Chung, N. Hutchins, M. P. Schultz, and K. A. Flack. Predicting the drag of rough surfaces. Annual Review of Fluid Mechanics, 53:439–471, 2021.
[5] K. A. Flack and D. Chung. Important parameters for a predictive model of k_s for zero pressure gradient flows. AIAA Journal, 60:5923–5931, 2022.
[6] M. A. Jouybari, J. Yuan, G. J. Brereton, and M. S. Murillo. Data-driven prediction of the equivalent sand-grain height in rough-wall turbulent flows. Journal of Fluid Mechanics, 912:A8, 2021.
[7] L. Chan, M. MacDonald, D. Chung, N. Hutchins, and A. Ooi. A systematic investigation of roughness height and wavelength in turbulent pipe flow in the transitionally rough regime. Journal of Fluid Mechanics, 771:743–777, 2015.
[8] P. Forooghi, A. Stroh, F. Magagnato, S. Jakirilić, and B. Frohnapfel. Toward a universal roughness correlation. ASME Journal of Fluids Engineering, 139:121201, 2017.
[9] K. A. Flack, M. P. Schultz, and J. M. Barros. Skin friction measurements of a systematically-varied roughness: probing the role of roughness amplitude and skewness. Flow Turbulence and Combustion, 104:317–329, 2019.
[10] A. E. Perry and P. N. Joubert. Rough-wall boundary layers in adverse pressure gradients. Journal of Fluid Mechanics, 17(2):193–211, 1963.
[11] J. M. Österlund, A. V. Johansson, H. M. Nagib, and M. H. Hites. A note on the overlap region in turbulent boundary layers. Physics of Fluids, 12(1):1–4, 2000.
[12] V. Vishwanathan, D. J. Fritsch, K. T. Lowe, and W. J. Devenport. History effects and wall-similarity of non-equilibrium turbulent boundary layers in varying pressure gradient over rough and smooth surfaces. International Journal of Heat and Fluid Flow, 102:109145, 2023.
[13] D. J. Fritsch, V. Vishwanathan, C. J. Roy, K. T. Lowe, and W. J. Devenport. Turbulence and pressure fluctuations in rough wall boundary layers in pressure gradients. Experiments in Fluids, 63:140, 2022.
[14] D. J. Fritsch. The effects of pressure gradient and roughness on pressure fluctuations beneath high Reynolds number boundary layers. PhD thesis, Virginia Tech, Aerospace and Ocean Engineering, 2022.
[15] V. Vishwanathan. The resolution and structure of high Reynolds number turbulent boundary layers over rough and smooth walls in pressure gradient. PhD thesis, Virginia Tech, Aerospace and Ocean Engineering, 2023.
[16] R. J. Volino and M. P. Schultz. Determination of wall shear stress from mean velocity and Reynolds shear stress profiles. Physical Review Fluids, 3:034606, 2018.
[17] R. J. Volino and M. P. Schultz. Effects of boundary layer thickness on the estimation of equivalent sandgrain roughness in zero pressure gradient boundary layers. Experiments in Fluids, 63:131, 2022.
[18] R. J. Volino and M. P. Schultz. Comparison of smooth- and rough-wall non-equilibrium boundary layers with favourable and adverse pressure gradients. Journal of Fluid Mechanics, 959:A35, 2022.
[19] R. J. Volino. Reynolds number dependence of zero pressure gradient turbulent boundary layers. ASME Journal of Fluids Engineering, 142:051303, 2020.
[20] R. J. Volino. Non-equilibrium boundary layer development in turbulent boundary layers with changing pressure gradients. Journal of Fluid Mechanics, 897:A2, 2020.
[21] N. Abderrahaman-Elena, C. T. Fairhill, and R. García-Mayoral. Modulation of near-wall turbulence in the transitionally rough regime. Journal of Fluid Mechanics, 865:1042–1071, 2019.
[22] H. Mulchadani and R. García-Mayoral. Roughness function and turbulent statis-

tics with increasing roughness size from direct numerical simulations. In 12th International Symposium on Turbulent Shear Flow Phenomena (TSFP12), number TSFP12, Osaka, Japan, July 2022.

[23] C. T. Fairhall, N. A. Abderrahaman, and R. García-Mayoral. The effect of slip and surface texture on turbulence over superhydrophobic surfaces. Journal of Fluid Mechanics, 861:88–118, 2019.

[24] W. Xie, C. T. Fairhall, and R. García-Mayoral. Resolving turbulence and drag over textured surfaces using texture-less simulations: the case of slip/no-slip textures, 2024.

[25] W. C. Reynolds and A. K. M. F. Hussain. The mechanics of an organized wave in turbulent shear flow. Part 3. Theoretical models and comparisons with experiments. Journal of Fluid Mechanics, 54(2):263–288, 1972.

[26] D. D. Wangsawijaya, R. Baidya, D. Chung, I. Marusic, and N. Hutchins. The effect of spanwise wavelength of surface heterogeneity on turbulent secondary flows. Journal of Fluid Mechanics, 894:A7, 2020.

[27] Z. Hantsis and U. Piomelli. Roughness effects on scalar transport. Physical Review Fluids, 5(2):114607, 2020.

[28] D. C. Wilcox. Turbulence Modeling for CFD. DCW Industries, first edition, 1994.

[29] D. C. Wilcox. Turbulence Modeling for CFD. DCW Industries, third edition, 2006.

[30] J. C. Kok. Resolving the dependence on freestream values for the k-ω turbulence model. AIAA Journal, 38(7):1292–1295, 2000.

[31] F. R. Menter. Two-equation eddy-viscosity turbulence models for engineering applications. AIAA Journal, 32(8):1598–1605, 1994.

[32] F. R. Menter, M. Kuntz, and R. Langtry. Ten years of industrial experience with the SST turbulence model. In Y Nagano, M J Tummers, and K Hanjalic, editors, Fourth International Symposium on Turbulence, Heat and Mass Transfer, volume 4, pages 625–632, New York, New York, 2003. Begell House.

[33] A. Hellsten and S. Laine. Extension of the k-ω SST turbulence model for flows over rough surfaces. In 22nd Atmospheric Flight Mechanics Conference, number AIAA Paper 97-3577, New Orleans, Louisiana, 1997.

[34] T. Knopp, B. Eisfeld, and J. B. Calvo. A new extension for k-ω turbulence models to account for wall roughness. International Journal of Heat and Fluid Flow, 30:54–65, 2009.

[35] B. Aupoix. Wall roughness modeling with k-ω SST model. In 12th International Symposium on Engineering Turbulence Modelling and Measurements, Marbella, Spain, 2014.

[36] B. Aupoix. A general strategy to extend turbulence models to rough surfaces: application to Smith's k-L model. ASME Journal of Fluid Engineering, 129(10):1245–1254, 2007.

[37] B. Smith. The k-$k\ell$ turbulence model and wall layer model for compressible flows. In 21st Fluid Dynamics, Plasma Dynamics and Lasers Conference, number AIAA Paper 90-1483, Seattle, Washington, 1990.

[38] F. R. Menter, Y. Egorov, and D. Rusch. Steady and unsteady flow modelling using the k-$\sqrt{k}L$ model. In Fifth International Symposium on Turbulence, Heat and Mass Transfer, volume 5, pages 403–406, New York, New York, 2006. Begell House.

[39] L. Eça, M. Kerkvliet, and S. L. Toxopeus. On the simulation of turbulent flows over rough walls using the RANS equations. In 24th Numerical Towing Tank Symposium (NuTTS), Zagreb, Croatia, 2022.

[40] P. A. Durbin, G. Medic, J. M. Seo, J. K. Eaton, and S. Song. Rough wall modification of two-layer k-ϵ. Journal of Fluids Engineering, 123(1):16–21, 2001.

[41] P. Spalart and S. Allmaras. One-equation turbulence model for aerodynamic flows. In 30$^{\text{th}}$ Aerospace Sciences Meeting, number AIAA Paper 92-439, Reno, Nevada, 1992.

[42] B. Aupoix and P. R. Spalart. Extensions of the Spalart-Allmaras turbulence model to account for wall roughness. In Fifth International Symposium on Engineering Turbulence Modelling and Measurements, volume 5, Amsterdam, 2002. Elsevier.

[43] B. Aupoix and P. R. Spalart. Extensions of the Spalart-Allmaras turbulence model to account for wall roughness. International Journal of Heat and Fluid Flow, 24(4):454–462, 2003.

[44] B. Eisfeld, C. Rumsey, and V. Togiti. Verification and validation of a second-moment-closure model. AIAA Journal, 54(5):1524–1541, 2006.

[45] L. Eça, M. Hoekstra, and H. Raven. Quantifying roughness effects by ship viscous flow calculations. In 28$^{\text{th}}$ Symposium on Naval Hydrodynamics, Pasadena, California, 2010.

[46] L. Eça and M. Hoekstra. Numerical aspects of including wall roughness effects in the SST k-ω eddy-viscosity turbulence model. Computers Fluids, 40(1):299–314, 2011.

[47] L. Eça, A. R. Starke, M. Kerkvliet, and H. Raven. On the contribution of roughness effects to the scaling of ship resistance. Journal of Ocean Engineering and Marine Energy, 8(3):539–551, 2022.

[48] D. J. Fritsch, V. Vishwanathan, C. J. Roy, K. T. Lowe, W. J. Devenport, Y. Nishi, T. Knopp, P. Ströer, A. Krumbien, R. D.Sandberg, C. Lav, R. E. Bensow, L. Eça, S. L. Toxopeus, M. Kerkvliet, M. Slama, and L. Bordier. Experimental and computational study of 2D smooth wall turbulent boundary layers in pressure gradient. In AIAA Science and Technology Forum, San Diego, California, January 2022.

[49] A. F. Mills and X. Hang. On the skin friction coefficient for a fully rough flat plate. ASME Journal of Fluid Engineering, 105:364–365, 1983.

[50] L. Eça, M. Kerkvliet, and S. L. Toxopeus. Comparison of RANS turbulence models for the simulation of smooth wall boundary-layers in pressure gradients at moderate and high Reynolds numbers. In 10$^{\text{th}}$ International Conference on Computational Methods in Marine Engineering (MARINE 2023), Madrid, Spain, 2023.

[51] D. J. Fritsch, V. Vishwanathan, C. J. Roy, K. T. Lowe, and W. J. Devenport. Modeling the surface pressure spectrum on rough walls in pressure gradients. ASME Journal of Fluids Engineering, 145(12):121301, 2023.

[52] J. Nikuradse. Laws of flow in rough pipes. Technical Report Technical Memorandum 1292, NACA, 1950.

[53] W. M. Kays and M. E. Crawford. Convective Heat and Mass Transfer. McGraw-Hill, New York, New York, third edition, 1993.

[54] P. A. Durbin and B. A. Petterson Reif. Statistical Theory and Modeling for Turbulent Flows. John Wiley, Hoboken, New Jersey, second edition, 2011.

[55] C. Meneveau. A note on fitting a generalised moody diagram for wall modelled large-eddy simulations. Journal of Turbulence, 21(11):650–673, 2022.

[56] B. J. McKeon and A. Sharma. A critical layer framework for turbulent pipe flow. Journal of Fluid Mechanics, 658:336–382, 2010.

[57] B. J. McKeon. The engine behind (wall) turbulence: perspectives on scale inter-

actions. Journal of Fluid Mechanics, 817:P1, 2017.

[58] R. Moarref, A. S. Sharma, J. A. Tropp, and B. J. McKeon. Model-based scaling and prediction of the streamwise energy intensity in high-Reynolds number turbulent channels. Journal of Fluid Mechanics, 734:275–316, 2013.

[59] R. Alvarez-Mejia and K. T. Christensen. Low-order representations of irregular surface roughness and their impact on a turbulent boundary layer. Physics of Fluids, 2(1):015106, 2010.

[60] J. Klewicki, R. Sandberg, T. Knopp, W. Devenport, D. Fritch, V. Vishwanathan, R. Volino, L. Eça, S. Toxopeus, and B. McKeon. On the physical structure, modeling and computation-based prediction of two-dimensional, smooth-wall turbulent boundary layers subjected to streamwise pressure gradients. submitted to Journal of Turbulence, 2024.